

Adsorption of Lead (II) from Aqueous Solution Using Adsorbents Obtained from Nanche Stone (*Byrsonima Crassifolia*)

Luis Armando Bernal-Jácome¹, Lizeth Olvera-Izaguirre¹, Marisol Gallegos García¹, Raúl Delgado-Delgado², Miguel Ángel Espinosa Rodríguez^{2*}

¹Programa de Maestría en Tecnología y Gestión del Agua. Facultad de Ingeniería, Universidad Autónoma de San Luis Potosí. Av. Dr. Manuel Nava No. 8 Zona Universitaria, C.P. 78290, San Luis Potosí, S.L.P. México.

²Programa Académico de Ingeniería Química de la Unidad Académica de Ciencias Básicas e Ingenierías, Universidad Autónoma de Nayarit. Ciudad de la Cultura Amado Nervo S/N, C.P. 63155, Tepic, Nayarit, México.

*Corresponding author: Miguel Ángel Espinosa Rodríguez, email: emiguel@uan.edu.mx

Received April 21st, 2020; Accepted September 13th, 2020.

DOI: <http://dx.doi.org/10.29356/jmcs.v64i4.1201>

Abstract. The removal capacity of Pb(II) present in aqueous solution was evaluated, using as a sorbent the nanche stone (*Byrsonima crassifolia*) naturally (NS), modified with citric acid (MNS) and as activated carbon (AC). The point of zero charge (pH_{PZC}) and the active sites (using the Boehm method and FTIR spectroscopy) were determined. The pH_{PZC} of NS, MNS and AC were in an acid range. The concentration of active sites of NS, MNS and AC were 0.1037, 0.1123 y 0.1404 mol/g, respectively. The infrared spectra (FTIR) detected the formation of acid functional sites associated with the phenol group, carboxylic acids and lactones. The adsorption capacity of lead ions using NS, MNS and AC increases with the increment of the pH of the solution from 3 to 5; nevertheless, at pH 5, precipitation of lead ions is observed. Due to the above, the evaluation of the three materials was carried out at pH 4. Comparing the maximum capacity of adsorption of Pb(II) on NS with respect to MNS and AC at pH 4, it was increased in 2.2 and 10 times, respectively. The chemical modification applied to precursor, as well as its formation to AC, improved their adsorption capacity due to a greater generation of acid sites. The experimental data were represented with the models of Langmuir, Freundlich and Prausnitz-Radke and the parameter values of these isotherms were estimated using a least-squares method which utilizes an optimization algorithm.

Keywords: Adsorption; nanche stone; Pb(II).

Resumen. Se evaluó la capacidad de remoción de Pb(II) presente en solución acuosa, utilizando como adsorbente el hueso de nanche (*Byrsonima crassifolia*) de forma natural (HN), modificado con ácido cítrico (HNM) y como carbón activado CA. Se determinaron el punto de carga cero ($pHPZC$) y los sitios activos (utilizando el método Boehm y espectroscopía FTIR). El $pHPZC$ del HN, HNM y CA estuvo en un rango ácido. La concentración de sitios ácidos del HN, HNM y CA fueron de 0.1037, 0.1123 y 0.1404 mol/g respectivamente. Los espectros infrarrojos (FTIR), detectaron la formación de sitios funcionales ácidos asociados al grupo fenol, ácidos carboxílicos y lactonas. La capacidad de adsorción del ion plomo con el HN, HNM y CA, aumentó al incrementarse el pH de la solución de 3 a 5; sin embargo, a pH 5, se observó precipitación de iones plomo. Debido a lo anterior, la evaluación de los tres materiales se realizó a pH 4. Comparando la máxima capacidad de adsorción de Pb(II) en el HN con respecto al HNM y al CA a pH 4, se incrementó en 2.2 y 10 veces, respectivamente. La modificación química aplicada al precursor, así como su formación a CA, amplió su poder de adsorción al desarrollarse una mayor cantidad de sitios activos ácidos. Los datos experimentales se representaron con los modelos de Langmuir, Freundlich y Prausnitz-Radke, y los

valores de los parámetros de estas isoterma fueron estimados usando un método de mínimos cuadrados que utiliza un algoritmo de optimización.

Palabras clave: Adsorción; hueso de nanche; Pb(II).

Introduction

In recent years, agricultural wastes have been used in adsorption processes for lead ion (Pb(II)) removal from aqueous solution. Several sources as cocoa pod, banana stem, rice husk, coconut husk, papaya and melon rind, soya waste, grape seeds, nut shells, moringa and cane bagasse have been used to remove Pb²⁺ [1-3].

An agricultural waste has a certain capacity for adsorption but if it is chemically modified, its adsorption capacity is increased through cation exchange. Citric acid has been used as oxidant agent to modify the surface chemistry of a precursor [1,4].

Furthermore, agricultural wastes have been used to obtain activated carbon (AC). The AC has result being a highly effective adsorbent for removal of a wide variety of organic and inorganic contaminants and metal ions in aqueous media. Activated carbon has been obtained from bamboo stalk, cane bagasse, olive stone, cherry stone, oil coconut stone, peach stone, nut shell, pine cone, acorn shell, coconut shell, tobacco waste, coffee waste, industrial tea waste, pistachio and walnuts wood, etc. [5-7].

The nanche tree or changunga (*Byrsonima crassifolia*) can grow wild or cultivated. It is localized in tropical and subtropical regions of Mexico, specifically in the gulf states: Tamaulipas, San Luis Potosí, Veracruz, Tabasco, Yucatán and Quintana Roo, and the states of the Pacific Mexican Coast: Sinaloa, Nayarit, Michoacán, Guerrero, Oaxaca and Chiapas. There are many species of this fruit, nevertheless the morphological characterization is very similar regarding the fruit (mesocarp), stone (endocarp) and seed [8, 9]. The nanche stone waste are generated by agroindustry and several satisfiers (food, medicinal, ornamental, fuel, tanning, coloring, beekeeping, fodder and timber) [10-12].

Activated carbon continues to be widely used for the removal of toxic compounds present in wastewater, so the search for low-cost precursors is convenient to streamline municipal and industrial water treatment processes, and if these materials come from agricultural waste, also helps to solve the problem of elimination of these [13].

A few years ago, several researchs have been carried out in order to improve the adsorptive properties of natural materials due to their low cost for removing heavy metals, being the main agent used, citric acid [13,14].

Recently, experimental designs have been proposed to improve the uptake properties of *Byrsonima crassifolia* biomass using a chemical modification with citric acid for the removal of heavy metals under competitive sorption conditions [14].

The aim of this work is to use the nanche stone in three different ways: 1) Nanche stone without treatment (NS), 2) modified nanche stone with citric acid (MNS) and 3) activated carbon obtained from the nanche stone (AC), to remove Pb(II) ions from aqueous solutions. The adsorption capacity of the three different treatments performed to precursor was analyzed in terms of the pH and lead concentration.

Experimental

Materials and Methods

Preparation of nanche stone

The nanche stone was washed with a 0.01 M hydrochloric acid (HCl) solution to remove the pulp (mesocarp) from the sample. Subsequently, removal of HCl from nanche stone was carried out using distilled water. The nanche stone was dried at 60 °C and the dry material was ground until to reach a particle size of 14

mesh. The ground nanche stone was used as raw material to obtain the following three adsorbents: nanche stone without treatment (NS), modified nanche stone (MNS) and activated carbon (AC).

Oxidation of nanche stone

The superficial chemistry of the ground nanche stone (NS) was modified using a 1 M citric acid ($C_6H_8O_7$) solution. A 50 mL solution of citric acid was added to each 10 g of ground nanche stone. The solution with the nanche stone grounded was heated at 55 °C during 2 h then cooled to reach the room temperature and drained. Subsequently, the nanche stone was dried in a stove at 50 °C for 24 h and at 120 °C for 3 h. The cold nanche stone was washed with distilled water to reach the neutral pH. Finally, the nanche stone was again dried at 50 °C during 24 h to be characterized and used in the experimental tests as MNS.

Carbonization and activation of nanche stone

The ground nanche stone (NS) was carbonized and activated in a tube furnace (Carbolite model MTF). The activation of the carbon was carried out chemically, using zinc chloride ($ZnCl_2$) as activating agent. The temperature and the optimal carbonization time were determined through a thermogravimetric analysis, obtaining values of 450 °C and 25 min, respectively. The impregnated material with activating agent was placed in the quartz tube of the furnace. The carbonization temperature, activation time, heat rate and nitrogen flow values were entered to the programmable control system of the furnace. Once the optimum temperature was reached, it remained constant for the determined time (25 min). AC was obtained with relationships: AC: $ZnCl_2$ 1.0:0.5; 1.0:1.0 and 1.0:1.5.

Determination of the pH_{PZC}

The adsorbent material was mixed with deionized water free of CO_2 . Carbon dioxide was completely removed from the deionized water by boiling during 20 min. A mixture of 1.0 g of adsorbent with 20 mL of deionized water was heated at 25 °C with constant agitation for 48 h. Finally, the pH of the solution was measured, corresponding to the pH_{PZC} .

Superficial chemistry (active sites)

The quantity of active sites of NS, MNS and AC was determined using the acid-base titration method proposed by Boehm [15]. A solution containing 0.3 g of adsorbent material, 20 mL of 1 M HCl solution and 20 mL of 1 M sodium hydroxide solution (NaOH) was prepared separately. The solutions were stirred during 120 h at 25 °C until an equilibrium was reached. At the end of the stirring time, each of the samples was filtered and the entire filtered volume was taken for neutralization. The total acid sites and total basic sites were neutralized with 1 M NaOH solution and 1 M HCl solution, respectively.

FTIR Characterization

Infrared spectra for the three adsorbents (NS, MNS and AC) were obtained using a Fourier transform infrared spectrometer (FTIR) (Thermo Scientific model Nicolette iS10 Smart iTR). The samples were analyzed in the mid-infrared region ($4000-400\text{ cm}^{-1}$) using the method of attenuated total reflectance.

Equilibrium adsorption isotherms

A lead standard solution with an initial concentration of 1,000 mg/L was prepared. The solution was prepared with lead nitrate [$Pb(NO_3)_2$], purity 99%, Merck brand graduated in 1 L of deionized water. Dilutions at different concentrations (10, 30, 50, 100 mg/L etc.) were made from this solution. 50 mL of the solutions with different concentrations of Pb^{2+} were added in 100 mL bottles. Subsequently, 1.0 g of adsorbent was added to each solution and pH was adjusted to 3, 4 and 5. The solutions were maintained at 25 °C with sporadic agitation for 7 days until an equilibrium was reached. The pH of all the mixtures was adjusted daily with NaOH and HNO_3 0.1 N as appropriate. Afterwards, mixtures were filtered to remove the adsorbent and Pb^{2+} concentration was determined by an ICP-OES spectrometer Thermo Scientific Model iCAP 7000.

The equilibrium data were analyzed in accordance with the Langmuir adsorption isotherm as:

$$q_e = \frac{q_{max}bCe}{1 + bCe} \quad (1)$$

where, q_e is the metal ion uptake (mg/g adsorbent), q_{max} is the maximum sorption capacity corresponding to complete monolayer coverage (mg/g), C_e is the equilibrium solute concentration (mg/L) and “ b ” is a constant relative to the energy of sorption (L/mg).

The Freundlich model:

$$q_e = kCe^{1/n} \quad (2)$$

being “ k ” Freundlich constant that is related to the adsorption capacity and “ $1/n$ ” is related to the adsorption intensity of the adsorbent.

And the Prausnitz-Radke model is represented by the following equation:

$$q_e = \frac{aCe}{1 + bCe^\beta} \quad (3)$$

where, a , b y β are constants of the Prausnitz-Radke isotherm.

The values of the isotherm constants were estimated using a least-squares method based on an optimization algorithm.

The adsorption capacity of the studied materials in the removal process of Pb(II) was calculated according to the mass balance (Equation 4):

$$q_\infty = \frac{V(C_{A0} - C_{A\infty})}{m} \quad (4)$$

where, q_∞ (metal solute uptake, mg/g adsorbent), V (solution volume, L), C_{A0} (initial solute concentration, mg/L), $C_{A\infty}$ (equilibrium solute concentration, mg/L) y m (mass of the adsorbent, g).

Results and discussion

Chemical characterization

The chemical characterization for nanche stone without treatment (NS), modified nanche stone (MNS) and activated carbon (AC) is presented in Table 1.

Table 1. Chemical characterization for of the adsorbent materials.

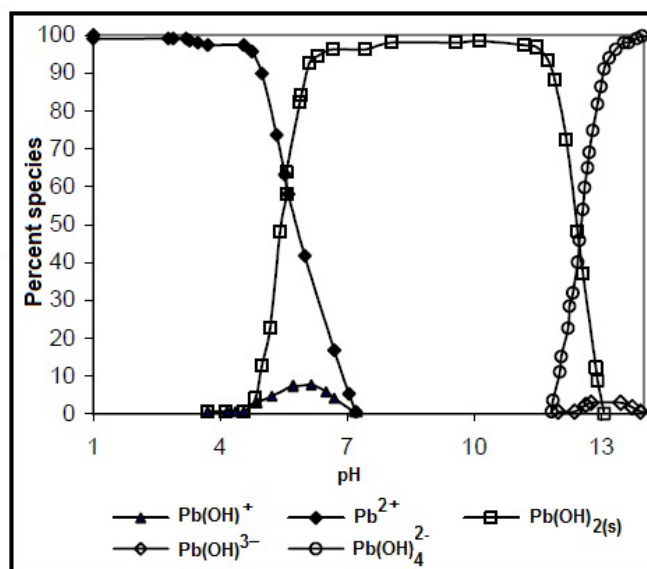
Material	Acid sites (mol/g)	Basic sites (mol/g)	pH _{PZC}
NS	0.1037	0.046	6.0
MNS	0.1123	0.042	5.6
AC	0.1404	0.044	5.9

According with Table 1, formation of acid sites was favored when NS is oxidized by citric acid, increasing significantly their concentration. This can be attributed to the fact that the surface of the adsorbent was modified, thereby increasing the presence of oxygenated groups [16]. The chemical modification has been used to increase the adsorption capacity of cations in contact with agricultural wastes [1].

In the case of carbon activation with ZnCl₂, the concentration of acid sites was further increased. The aqueous solutions of ZnCl₂ present an acid character due to the Zn²⁺ ions act as a Lewis acid, thus the ZnCl₂ acts as a dehydration agent during the carbonization process, resulting in charring and aromatization reactions and development of the pore structure. Also, molecular hydrogen is evolved from the hydroaromatic structure of the precursor and leaves behind some sites for reaction [17-19].

With reference to pH_{PZC}, the results of the NS, MNS and AC are maintained in acidic zones, which is consistent with the result of the concentration of acid sites, presenting a significant decrease in the zero charge point when the NS is oxidized with citric acid. The pH_{PZC} values obtained for MNS and AC indicate the acidic nature of the adsorbent materials due to the treatment applied, which caused the insertion of oxygenated groups. The pH_{PZC} value is the point at which the superficial functional groups do not contribute to the pH of the solution [1].

On the other hand, the speciation diagram of the lead obtained with the Pb(NO₃)₂ salt, showed the pH range with which we worked (Fig. 1). A predominance of Pb²⁺ at pH 5.5 can be observed in Fig. 1, while at pH 5.0 the precipitate formation of lead hydroxide [Pb(OH)_{2(s)}] and the soluble specie [Pb(OH)⁺] starts occurring. Also, at pH between 12 and 13, the most common species of hydroxide are Pb(OH)₄²⁻ y Pb(OH)₃⁻. Based on the speciation diagram, it was decided to analyze the removal of Pb²⁺ at pH 3, 4 and 5.

**Fig. 1.** Lead species as a function of pH. [20]

According to Fig. 1, the ions Pb²⁺ predominates at pH < 5.5, which indicates a pH < pH_{PZC} (Table 1). It is assumed, then, that H⁺ ions are released from the surface of the solid, while being negatively charged; this,

in turn, favors the adsorption of the lead ion. At $\text{pH} > \text{pH}_{\text{PZC}}$ the functional groups of the adsorbent surface are protonated. Also known that the point of zero charge (pH_{PZC}), which is indicative of the types of active centers on the surface and the adsorption mobility of the surface, is an important factor in adsorption processes [21, 22].

On the other hand, at $\text{pH} > \text{pH}_{\text{PZC}}$, the hydroxylated species affect the adsorption process, particularly the $\text{Pb}(\text{OH})_{2(s)}$ that starts to precipitate on the adsorbent surface, and consequently the adsorption of lead ions decreases. These results are in correspondence with those reported by other authors [1, 20, 23, 24].

FTIR Characterization

Fig. 2 shows the infrared spectra obtained for NS, MNS and AC. Peaks are observed that are characteristic of acidic functional groups which sequester heavy metals. Three important bands can be noticed: 1) the band between 3200 and 3600 cm^{-1} which is associated to phenol group (O-H), 2) the band from 2800 to 3100 cm^{-1} related to carboxylic acid groups (R-COOH), and 3) the band between 1600 and 1800 cm^{-1} related to vibrations of lactone groups (C=O) [21, 22, 25]. According to Fig. 2, the intensity of peaks defined above was higher for AC in comparison with those for NS and MNS. This suggests an increment in the quantity of phenolic and carboxylic groups.

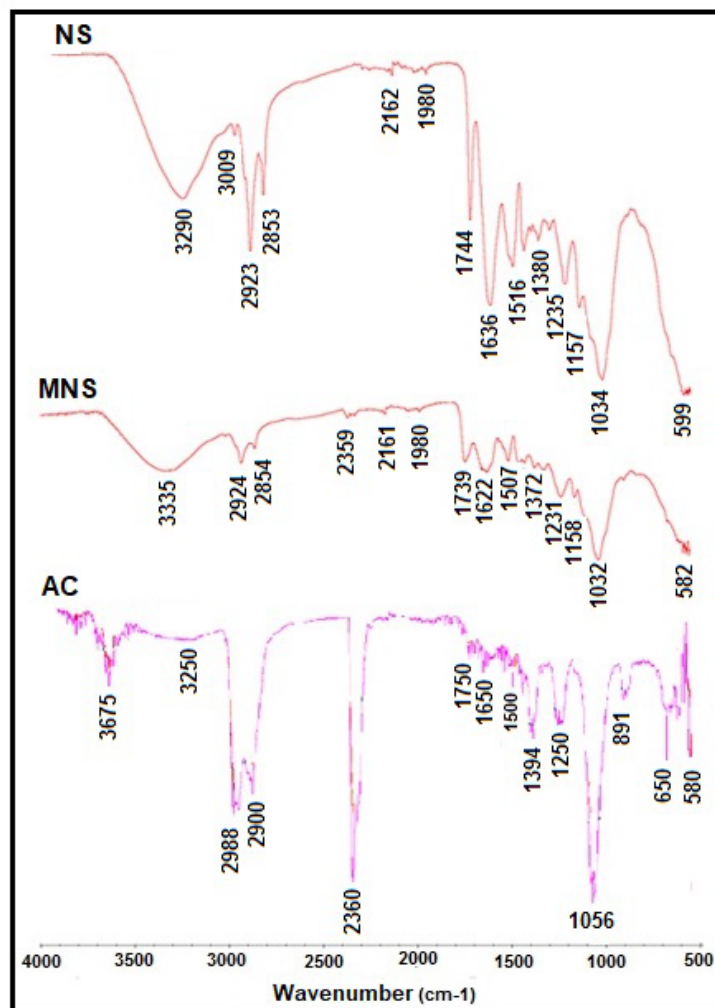


Fig. 2. Infrared spectra of NS, MNS and AC.

Equilibrium Adsorption Isotherms

Table 2 shows the results obtained from the absorbed mass of Pb^{2+} for each gram of NS, represented through the Langmuir, Freundlich and Prausnitz-Radke models.

Table 2. Results of the mathematical models at pH 3, 4, and 5 for NS.

pH	Ce (mg/L)	q _{exp} (mg/g)	q _{Langmuir} (mg/g)	% Desv	q _{Freundlich} (mg/g)	% Desv	q _{Prausnitz} (mg/g)	% Desv
3	8.80	1.19	1.00	18.73	0.75	57.17	1.16	1.98
	18.90	1.64	1.91	14.24	1.62	0.75	1.85	11.64
	21.80	2.25	2.13	5.68	1.87	20.27	2.05	10.13
	43.80	3.48	3.46	0.60	3.76	7.47	3.49	0.42
4	11.10	0.79	1.73	54.46	1.47	46.09	0.79	0.11
	15.90	2.15	2.28	5.47	2.11	1.90	2.13	0.71
	26.50	3.46	3.23	7.11	3.51	1.33	3.61	4.10
	33.90	4.73	3.74	26.57	4.49	5.33	4.63	2.36
5	2.40	1.23	1.97	37.53	1.95	37.14	1.93	36.09
	4.80	4.17	3.62	15.29	3.49	19.63	3.44	21.23
	9.70	6.44	6.35	1.44	6.31	2.12	6.31	2.11
	11.45	7.00	7.15	2.20	7.25	3.44	7.28	3.87

According to Table 2, the percentage of standard deviation for the Langmuir and Prausnitz-Radke models indicated the best fits to the experimental data for all pH studied. However, the adjustment of the Freundlich model was comparable to the Langmuir and Prausnitz-Radke models at pH 5. Fig. 3, 4 and 5 show the experimental and predicted dependence of the mass of absorbed lead (q) on equilibrium concentration (Ce) for pH 3, 4 and 5 using the models described above (Table 2).

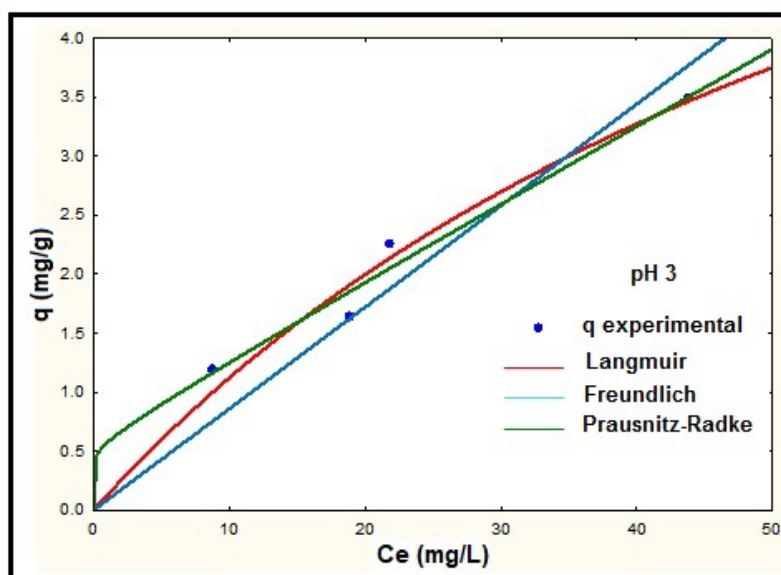


Fig. 3. Adsorption isotherms of NS at pH 3.

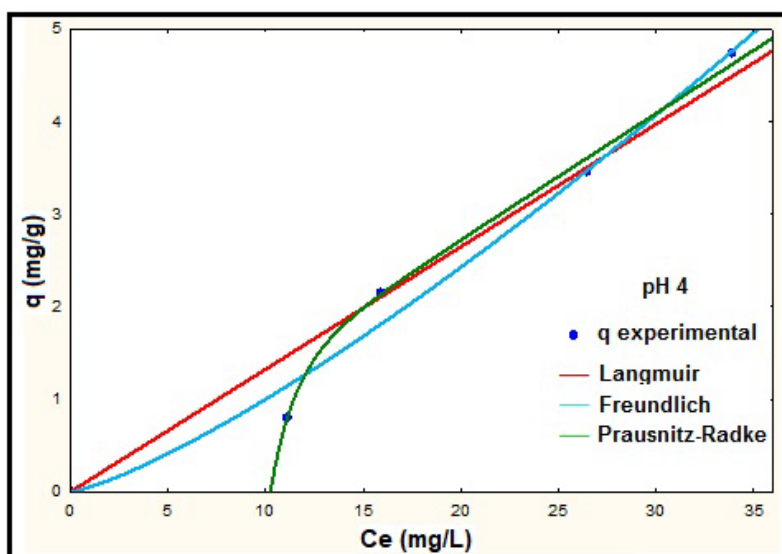


Fig. 4. Adsorption isotherms of NS at pH 4.

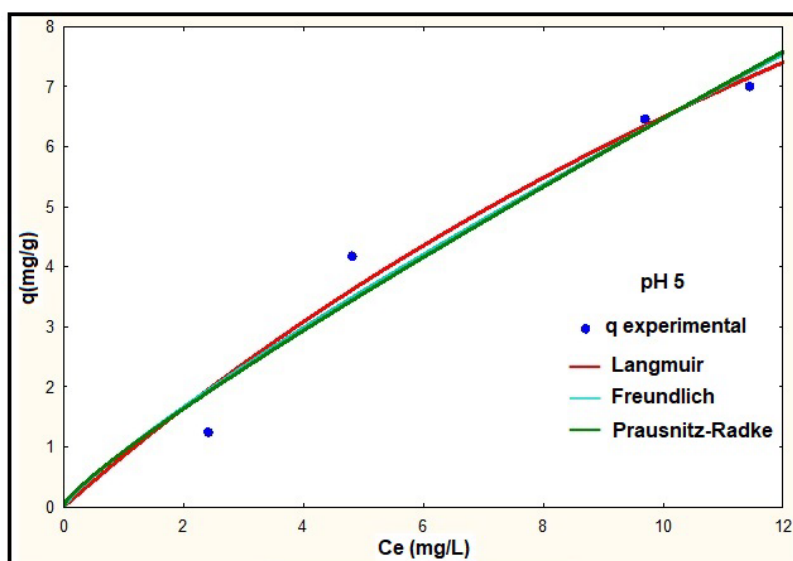


Fig. 5. Adsorption isotherms of NS at pH 5.

According to the results showed in Fig. 3, 4 and 5 it is observed that at higher pH the adsorbed mass of lead increases, presenting the best removal efficiencies at pH 5. The best fit to the experimental data was presented by the Langmuir model at all pH studied. On the other hand, the isotherm for the Prausnitz-Radke model was not fit properly at pH 4. Thus, a representation of isotherms of equilibrium using the Langmuir model was carried out and it is showed in Fig. 6.

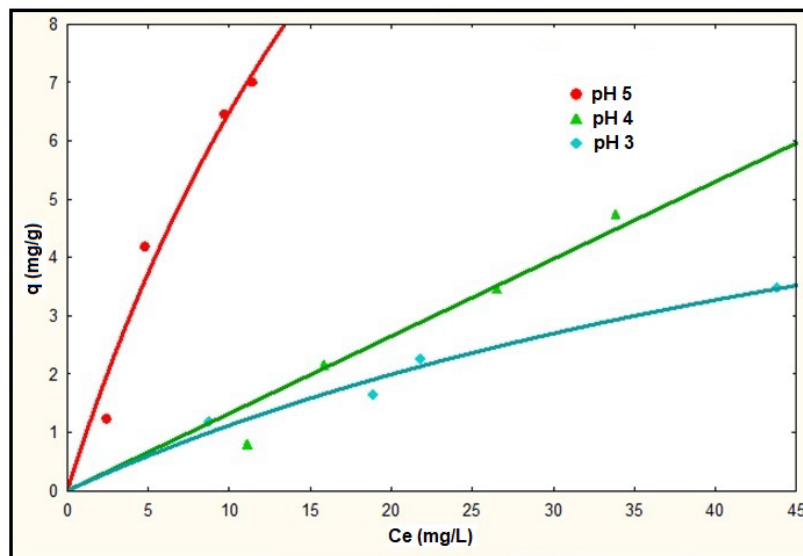


Fig. 6. Adsorption isotherms of NS using the Langmuir model.

The greatest adsorption capacity of lead in aqueous solution was obtained at pH 5, as can be observed in Fig. 6, however according to the speciation diagram (Fig. 1), the Pb^{2+} ion begins to precipitate at pH 5; this was observed during the adsorption tests, so it was decided to carry out the investigation at pH 4. Therefore, the experimental tests using the MNS was carried out at pH 4. These results were compared with those obtained using NS and they are shown in Fig. 7.

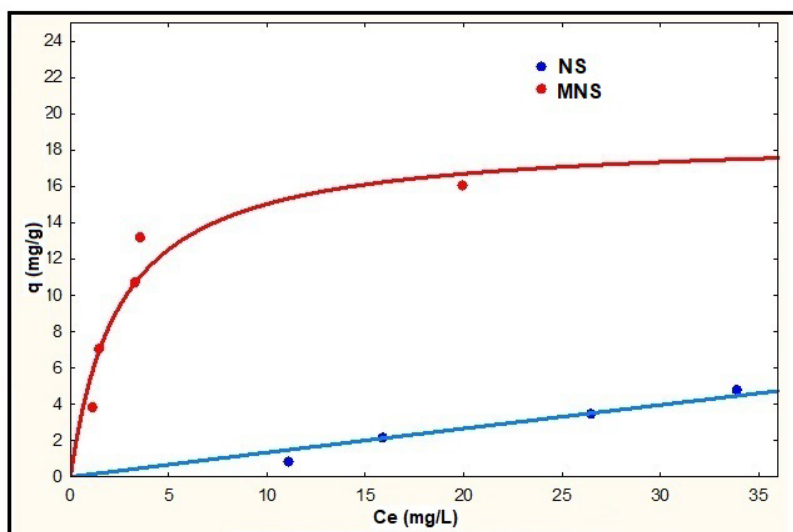


Fig. 7. Langmuir models for NS and MNS at pH 4.

The results represented in Fig. 7 show that MNS has a higher adsorption capacity than NS; the oxidation of NS with citric acid decreased the pH_{pzc} (Table 1) and therefore modified the surface chemistry of the adsorbent obtaining a greater number of acidic active sites that impacted the adsorption capacity of the lead ion [16].

Finally, equilibria parameters for the AC were obtained using different ratios of adsorbent material and activating agent (AC:ZnCl₂). These results, shown in Table 3, were taken as a base in the determination of the amount of AC used for the lead adsorption tests at pH 4.

Table 3. Results of mathematical models at pH 4 for AC.

AC:ZnCl ₂	Ce (mg/L)	q _{exp} (mg/g)	q _{Langmuir} (mg/g)	% Desv	q _{Freundlich} (mg/g)	% Desv	q _{Prausnitz} (mg/g)	% Desv
1.0:0.5	1.10	20.13	13.98	43.94	23.03	12.58	17.54	14.73
	5.55	35.66	43.54	18.10	41.58	14.23	40.19	11.27
	6.10	52.25	45.85	13.96	43.13	21.13	41.94	24.58
	18.30	64.09	68.68	6.69	64.31	0.34	63.59	0.78
	36.60	82.16	78.61	4.52	82.96	0.96	80.27	2.36
1.0:1.0	1.30	23.33	26.56	12.17	33.14	29.59	26.57	12.20
	1.80	36.11	32.14	12.10	35.96	0.42	32.20	12.16
	5.90	48.14	56.77	15.21	50.44	4.56	57.11	15.72
	6.60	66.94	58.95	13.00	52.16	28.34	59.30	12.89
	32.00	77.25	77.54	0.30	81.37	5.07	77.44	0.25
1.0:1.5	0.80	18.56	21.36	13.10	26.50	29.95	11.67	59.04
	1.55	36.06	32.24	11.84	31.75	13.56	15.66	130.21
	6.00	50.76	53.20	4.58	45.71	11.06	26.14	94.22
	20.00	64.23	63.28	1.51	63.41	1.30	32.90	95.25
	25.60	64.45	64.35	0.15	67.55	4.60	32.29	99.58

The results of Table 3 show that the best fit to the experimental data based on the percentage of standard deviation was for the Freundlich model using an AC:ZnCl₂ ratio of 1.0:0.5, while for AC:ZnCl₂ ratios of 1.0:1.0 and 1.0:1.5 was for the Langmuir model. However, according to the adsorption capacity at equilibrium, the lowest lead removal efficiency occurred with the 1.0: 1.5 ratio, while with the ratio 1.0: 0.5 and 1.0: 1.0 they were similar, which is also observed in Fig. 8. Considering the above two AC:ZnCl₂ ratios, the best adjustment was obtained using the Langmuir model at an AC:ZnCl₂ ratio of 1.0:1.0. In this context, Fig. 8 shows the Pb²⁺ adsorption isotherms at pH 4 with the Langmuir model for the different AC-ZnCl₂ ratios.

Considering the results shown in Table 3 and Fig. 8, in Table 4, the results of the adsorption equilibrium at pH 4 are presented with the Langmuir model for NS, MNS and AC (1:1), same as are represented in Fig. 9.

The results represented by the Langmuir isotherms of Fig. 9, show an increase in the adsorption capacity with the AC produced from the nanche stone (NS). Making a comparison of the adsorbed mass of Pb²⁺ per gram of adsorbent using the values of q_{max} shown in Table 4, the adsorption capacity increases 2.2 and 10 times compared with MNS and with AC (1:1), respectively.

This significant increase in the adsorption of the Pb²⁺ ion with AC with respect to NS and MNS, is due to the fact that there was a greater formation of acid sites, as detailed in chemical characterization and FTIR, but the generation of interspaces in the AC is also assumed due to the formation of pores and greater superficial area. The increase of the porosity could be attributed to the expansion (swelling) of molecular structure of cellulose contained in the carbon by the action of activation with ZnCl₂ [19,26]. Agricultural residues contain high levels of lignocellulosic material (cellulose, hemicellulose and lignin), which is the raw material for the synthesis of activated carbon [25,27]. Other studies have found that the activation of carbon with ZnCl₂ increase its superficial area and pore volume favoring the adsorption process [19,27-29].

In Table 5 presented results referent to the maximum adsorption capacity (q_{max}) of the Pb²⁺ ion in aqueous solution with agricultural wastes, modified agricultural wastes and AC elaborated from lignocellulosic material.

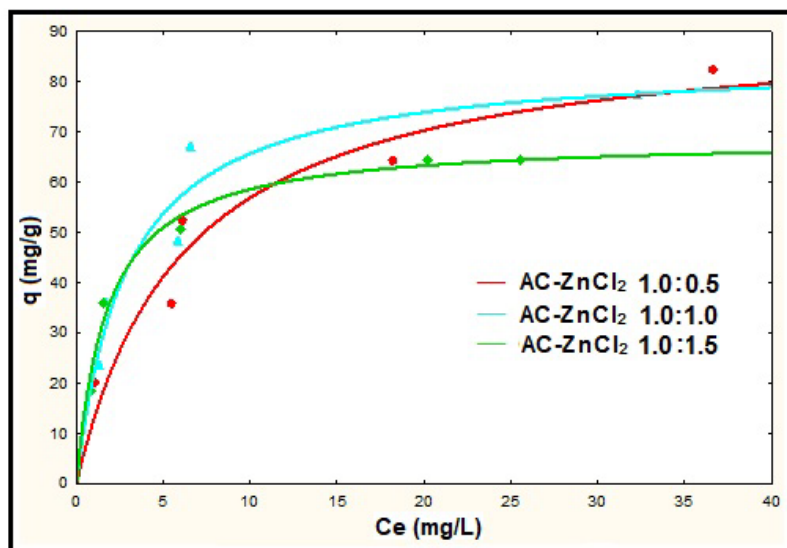


Fig. 8. Langmuir models for AC:ZnCl₂ ratios at pH 4.

Table 4. Langmuir model results and parameters at pH 4 for NS, MNS and AC.

Adsorbent	pH	Ce (mg/L)	q _{exp} (mg/g)	q _{Langmuir} (mg/g)	% Desv	Parameters of the model	
						q _{max}	b
NS	4	11.1	0.79	1.73	54.46	8.53	0.023
		15.9	2.15	2.28	5.47		
		26.5	3.46	3.23	7.11		
		33.9	4.73	3.74	26.57		
MNS	4	1.16	3.81	5.94	35.76	18.78	0.40
		1.45	7.02	6.91	1.59		
		3.33	10.66	10.73	0.60		
		3.57	13.17	11.05	19.20		
		19.95	16.03	16.69	3.92		
AC (1:1)	4	1.31	23.33	26.56	12.17	84.38	0.35
		1.76	36.11	32.14	12.37		
		5.88	48.14	56.77	15.21		
		6.62	66.94	58.95	13.56		
		32.40	77.25	77.54	0.38		

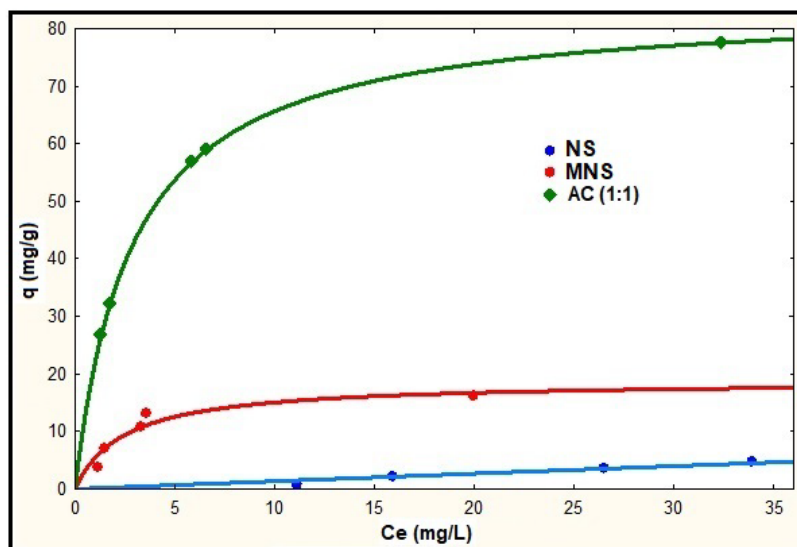


Fig. 9. Langmuir models for NS, MNS and AC:ZnCl₂ (1:1) at pH 4

Table 5. Comparison of the maximum adsorption capacity (q_{\max}) of Pb²⁺ with different adsorbents

Adsorbent	q_{\max} mg/g	References
Agricultural wastes		
Almond shell	2.00	[30]
Cashew nut shell	1.38	[31]
Walnut shell	9.91	[32]
Peach stone	0.0023	[33]
Apricot stone	0.0013	[33]
Olive stone	3.455	[34]
Hazelnut shell	16.23	[35]
Almond shell	5.43	[35]
Modified agricultural wastes		
Modified cashew nut shell with H ₂ SO ₄	8.73	[25]
Modified walnut shell with HCl	2.97	[36]
Modified walnut shell with NaOH	7.79	[36]
Modified coconut shell with H ₂ SO ₄	24.24	[37]
Modified peanut husk with H ₂ SO ₄	4.66	[38]
AC produced from agricultural wastes		
AC developed from peanut shell	59.00	[22]
AC developed from dinde stone	92.90	[22]
AC with H ₃ PO ₄ developed from olive stone	148.77	[39]
AC with H ₂ O ₂ developed from coconut shell	65.00	[40]
AC with H ₂ SO ₄ developed from jujube stone	71.43	[41]
AC with H ₂ SO ₄ developed from apricot stone	21.38	[42]
AC with KOH developed from olive stone	22.37	[43]
AC with H ₃ PO ₄ developed from date stone	11.85	[44]
AC with H ₂ SO ₄ developed from peach stone	19.43	[45]
AC with ZnCl ₂ developed sea-buckthorn stone	25.91	[46]
AC with H ₃ PO ₄ developed sea-buckthorn stone	51.81	[46]
AC with KOH developed from cashew nut shell	28.90	[47]

AC with H ₃ PO ₄ developed from peanut shell	35.46	[48]
AC with Zn Cl ₂ developed from hazelnut husk	13.05	[49]
Nanche stone	8.53	This study
Modified nanche stone with citric acid	18.78	This study
AC with ZnCl ₂ developed from nanche stone	84.38	This study

With reference to Table 5, the maximum adsorption capacity (q_{\max}) of Pb²⁺ obtained in this research work for the NS, MNS and AC is within the range of those obtained by other researchers with other agricultural residues; even in some cases, with higher adsorption capacity.

Conclusions

Three different adsorbents (NS, MNS and AC) obtained from nanche stone (*Byrsonima crassifolia*) were effective in the removal of Pb²⁺ ions. The pH_{pzc} of adsorbents (NS = 6.0; MNS = 5.6; AC = 5.9) was determined in the acid range favoring cation adsorption. Moreover, the main functional groups found in the adsorbents were carboxylic, phenol and lactone groups which contribute to the adsorption of heavy metals. The above is due to two factors: electrostatic interactions between the ions and the adsorbent surface, and specific chemical interactions among the ions and the surface complexes.

The pH of the solution had a significant effect over the lead ions adsorption because it determined the adsorbent surface charge, ionization grade and metal ion speciation.

Results indicated that it is feasible to improve the adsorption of this metal ion in aqueous solution modifying the nanche stone, initially with citric acid, observing that the adsorption capacity increased 2.2 times. This agricultural waste is the first time that it was used as a precursor to obtain activated carbon, improving the adsorption capacity 10 times demonstrating that it can be an economically viable alternative.

References

1. Emenike, P.; Omole, D.; Ngene, B.; Tenebe, I. *Global J. Environ. Sci. Manage.* **2016**, *2*, 411-442. <https://dx.doi.org/10.22034/gjesm.2016.02.04.010>
2. Sulyman, M.; Namiesnik, J.; Gierak, A. *Pol. J. Environ. Stud.* **2017**, *26*, 479-510. <https://dx.doi.org/10.15244/pjoes/66769>
3. Tejada, C.; Bonilla, H.; Pino, J.; Villabona, A.; Ortega, R. *Rev. Mex. Ing. Quím.* **2020**, *19*, 1413-1423. <https://doi.org/10.24275/rmiq/IA1101>
4. Zhu, B.; Fan, T.; Zhang, D. *J. Haz. Mat.* **2008**, *153*, 300-328. <https://doi.org/10.1016/j.jhazmat.2007.08.050>
5. Ozdemir, I.; Sahin, M.; Orhan, R.; Erdem, M. *Fuel Process. Technol.* **2014**, *125*, 200-206. <http://dx.doi.org/10.1016/j.fuproc.2014.04.002>
6. Obayomi, K. S.; Bello, J. O.; Nnoruka, J. S.; Adediran A. A.; Olajide, P.O. *Cogent Eng.* **2019**, *6*, 1-17. <https://doi.org/10.1080/23311916.2019.1687274>
7. Malekian, F.; Ghafourian, H.; Zare, K.; Sharif, A. A.; Zamani, Y. *J. Mex. Chem. Soc.* **2019**, *63*, 120-129. <http://dx.doi.org/10.29356/jmcs.v63i2.666>
8. Medina, R.; Salazar, S.; Gómez, J. *HortScience* **2004**, *39*, 1070-1073. <https://doi.org/10.21273/HORTSCI.39.5.1070>

9. Bayuelo, J.; Lozano, J.; Ochoa, I. *Rev. Fitotec. Mex.* **2006**, 29, 31-36.
10. Caballero, A.; Vela, G.; Pérez, J.; Escobar, R.; Ballinas, J. *Etnobiología* **2012**, 10, 50-55.
11. Guzmán, A.; Cruz, E.; Miranda, C. *Rev. Mex. Cien. For.* **2013**, 4, 82-89.
<https://doi.org/10.29298/rmcf.v4i20.372>
12. Medina, R.; Ibarra, M. E.; González, J. G.; Salazar, S. *Rev. Venez. Cienc. Tecnol. Aliment.* **2017**, 8, 45- 56. <https://sites.google.com/site/1rvcta>
13. Leyva, R.; Bernal, L. A.; Acosta, I. *Sep. Purif. Technol.* **2005**, 45, 41-49.
<https://doi.org/10.1016/j.seppur.2005.02.005>
14. Monroy, J.; Mendoza, D. I.; Bonilla, A.; Pérez, M. A. *Int. J. Environ. Sci. Technol.* **2015**, 12, 2867–2880. <https://doi.org/10.1007/s13762-014-0685-x>
15. Goertzen, S.; Thériault, K.; Oickle, A.; Tarasuk, A.; Andreas H. *Carbon* **2010**, 48, 1252-1261.
<https://doi.org/10.1016/j.carbon.2009.11.050>
16. Prado, M. A.; Arruda, S. M.; Ulson, A. A. *J. Clean. Prod.* **2014**, 65, 342-349.
<http://dx.doi.org/10.1016/j.jclepro.2013.08.020>
17. Chen, R.; Li, L.; Liu, Z.; Lu, M.; Wang, C.; Li, H.; Ma, W.; Wang, S. *J. Air Waste Manage. Assoc.* **2017**, 67, 713-724. <http://dx.doi.org/10.1080/10962247.2017.1280560>
18. Hock, P. E.; Ahmad, M. A. *Acta Chimica Slovaca* **2018**, 11, 99-106. <https://doi.org/10.2478/acs-2018-0015>
19. Heidarinejad, Z.; Hadi, M.; Heidari, M.; Javedan, G.; Ali, I.; Sillanpää, M. *Environ. Chem. Lett.* **2020**, 18, 393-415. <https://doi.org/10.1007/s10311-019-00955-0>
20. Giraldo, L.; Moreno, J. C. *Braz. J. Chem. Eng.* **2008**, 25, 143-151. <https://doi.org/10.1590/S0104-66322008000100015>
21. Wang, G.; Zhang, S.; Yao, P.; Chen, Y.; Xu, X.; Li, T.; Gong, G. *Arab. J. Chem.* **2018**, 11, 99-110.
<http://dx.doi.org/10.1016/j.arabjc.2015.06.0117>
22. Tasar, S.; Özer, A. *Pol. J. Environ. Stud.* **2020**, 29, 293-305. <https://doi.org/10.15244/pjoes/103027>
23. Singh, J.; Ali, A.; Prakash, V. *Int. J. Environ. Sci. Technol.* **2014**, 11, 1759-1770.
<https://doi.org/10.1007/s13762-013-0326-9>
24. Shi, B.; Zuo, W.; Zhang, J.; Tong, H.; Zhao, J. *J. Environ. Qual.* **2016**, 45, 984-992.
<https://doi.org/10.2134/jeq2014.12.0533>
25. Nuithitikul, K.; Phromrak, R.; Saengngoen, W. *Sci. Rep.* **2020**, 10, 1-14.
<https://doi.org/10.1038/s41598-020-60161-9>
26. Bedia, J.; Peñas, M.; Gómez, A.; Rodríguez, J. J. *Carbon Res.* **2020**, 6, 1-25.
<https://doi.org/10.3390/c6020021>
27. Subha, R.; Namasivayam, C. *Indian J. Chem. Technol.* **2009**, 16, 471-479.
<http://nopr.niscair.res.in/handle/123456789/6711>
28. Acharya, J.; Sahu, J.; Mohanty, C.; Meikap, B. *Chem. Eng. J.* **2009**, 149, 249-262.
<https://doi.org/10.1016/j.cej.2008.10.029>
29. Angin, D. *Fuel* **2014**, 115, 804-811. <http://dx.doi.org/10.1016/j.fuel.2013.04.060>
30. Obike, A. I.; Igwe, J. C.; Emeruwa C. N.; Uwakwe, K. J. *J. Appl. Sci. Environ. Manage.* **2018**, 22, 182-190. <https://doi.org/10.4314/jasem.v22i2.5>
31. Siripatana, C.; Khuenpetch, A.; Phromrak, R.; Saengngoen, W.; Nuithitikul, K. *J. Eng. Applied Sci.* **2017**, 12, 1819-1824.
32. Celebi, h.; Gök, O. *Int. J. Environ Res.* **2017**, 11, 83-90. <https://doi.org/10.1007/s41742-017-0009-3>
33. Saka, C.; Sahin, Ö.; Masuk, M. *Int. J. Environ. Sci. Technol.* **2012**, 9, 379-394.
<https://doi.org/10.1007/s13762-012-0041-y>

34. Martín, M. A.; Rodríguez, I. I.; Blázquez, G.; Calero, M. *Desal.* **2011**, 278, 132-140. <https://doi.org/10.1016/j.desal.2011.05.016>
35. Bulut, Y.; Tez, Z. *J. Haz. Mat.* **2007**, 149, 35-41. <https://doi.org/10.1016/j.jhazmat.2007.03.044>
36. Wolfová, R.; Pertile, E.; Fecko P. *J. Environ. Chem. Ecotoxicol.* **2013**, 5, 159-167. DOI: 10.5897/JECE09.025
37. Singha, B.; Kumar, S. *Environ. Sci. and Pollut. Res.* **2012**, 19, 2212-2226. <https://doi.org/10.1007/s11356-011-0725-8>
38. Li, Q.; Zhai, J.; Zhang, W.; Wang, M.; Zhou J. *J. Haz. Mat.* **2007**, 141, 163-167. <https://doi.org/10.1016/j.jhazmat.2006.06.109>
39. Saleem, J.; Bin, U.; Hijab, M.; Mackey, H.; McKay, G. *Biomass Conv. Bioref.* **2019**, 9, 775-802. <https://doi.org/10.1007/s13399-019-00473-7>
40. Jahangard, A.; Sohrabi, M.; Beigmohammadi, Z. *Iran. J. Toxicol.* **2016**, 10, 23-29. <https://doi.org/10.29252/arakmu.10.6.23>
41. Bouchelkia, N.; Mouni, L.; Belkhiri, L.; Bouzaza, A.; Bollinger, J.; Madani, K. *Separ. Sci. Technol.* **2016**, 51, 1645-1653. <https://doi.org/10.1080/01496395.2016.1178289>
42. Mouni, L.; Belkhiri, L.; Zouggaghe, F.; Tafer M. *Desal. Water Treat.* **2014**, 52, 6412-6419. <https://doi.org/10.1080/19443994.2013.812992>
43. Alslaibi, T.; Abustan, I.; Ahmad, M.; Abu, A. *Desal. Water Treat.* **2014**, 52, 7887-7897. <https://doi.org/10.1080/19443994.2013.833875>
44. Chaouch, N.; Ouahrani, M.; Laouini, S. *Orient. J. Chem.* **2014**, 30, 1317-1322. <http://dx.doi.org/10.13005/ojc/300349>
45. Ahmed, S.; Mohammad, S. *Mycopath* **2014**, 12, 87-93.
46. Mohammadi, S.; Karimi, M.; Afzali, D.; Mansouri, F. *Desal.* **2010**, 262, 86-93. <https://doi.org/10.1016/j.desal.2010.05.048>
47. Tangjuank, S.; Insuk, N.; Tontrakoon, J.; Udeye, V. *Int. J. Chem. Mol. Nucl. Mat. Metall. Eng.* **2009**, 3, 221-227. <https://doi.org/10.5281/zenodo.1074763>
48. Tao, X.; Xiaoqin, L. *Chin. J. Chem. Eng.* **2008**, 16, 401-406. [https://doi.org/10.1016/S1004-9541\(08\)60096-8](https://doi.org/10.1016/S1004-9541(08)60096-8)
49. Imamoglu, M.; Tekir, O. *Desal.* **2008**, 228, 108-113. <https://doi.org/10.1016/j.desal.2007.08.011>